Magnon and acoustic-phonon light scattering from Bi-doped yttrium iron garnet

P. X. Zhang,* D. J. Lockwood, and H. J. Labbé
Institute for Microstructural Sciences, National Research Council of Canada, Ottawa, Ontario, Canada K1A 0R6
(Received 29 March 1993)

Light scattering in Bi-substituted yttrium iron garnet has revealed different excitation-wavelength-dependent cross sections for the acoustic phonons and magnons. Analysis of the magnon and phonon frequencies showed a quadratic and linear dependence, respectively, with wave vector and models for these results indicate that the spin-wave stiffness constant is increased, while the sound velocity is reduced, by the substitution of Y with Bi. With the reduction of excitation wavelength, which is accompanied by an increase in the light absorption, a line broadening, and finally a double peak with a continuous band in between, is observed in magnon scattering.

I. INTRODUCTION

Bismuth-substituted yttrium iron garnet (Bi-YIG) crystals are now widely used as magneto-optical materials because of their high figures of merit.[1,2] Although Bi^{3+} is a diamagnetic ion, its presence, however, increases the Faraday rotation dramatically and also the Curie point T_C of the magnetic material.[3] The physical origins of these effects are not yet clear. In earlier Brillouin scattering experiments on Bi-YIG, only magnon scattering was observed.[4] Why the acoustic phonons, which normally exhibit a cross section similar to, or larger than that of the magnon,[5] were not observed is another interesting question. From previous light-scattering studies of cubic YIG,[5,6] it has been shown that both dissipative and nondissipative magneto-optical effects influence the magnon intensity, as revealed through the ratio of the Stokes and anti-Stokes intensities. Thus, it is interesting in light-scattering experiments to study the effects of Bi doping in YIG not only on the magnon frequency but also on the magnon intensity.

In this paper we report a detailed study by light-scattering spectroscopy of a Bi-YIG single crystal. We have measured the magnons and acoustic phonons at a wider range of laser exciting frequencies and with higher applied magnetic field than in the earlier Brillouin scattering study.[4] It was found that the scattering intensity of the magnons increases gradually, while that of the longitudinal-acoustic (LA) phonon decreases markedly and eventually becomes undetectable with an increase of the laser frequency. This indicates that there is a special light-scattering resonance occurring in these magnetic materials, which enhances the intensity of the magnons while suppressing that of the LA phonons. At the same time, the linewidth of the magnon peak shows a broadening and, at higher resolution, an additional small peak is observed at the lower-frequency side of the main one.

II. EXPERIMENT

The Bi-substituted YIG single crystals were grown by the flux method in a Pt crucible.[7] A small and shiny single crystal of approximate size $1\times1\times1$ mm^3 and with (001), (110), and (1$\bar{1}$0) faces was selected as the sample for this study. The sample composition was analyzed by energy dispersive x-ray analysis and was found to be $Bi_{0.41}Y_{2.59}Fe_5O_{12}$. For this composition, $T_C \approx 560$ K.[7] For the light-scattering measurements, the as-grown (001) surface of the crystal was gently polished with 1 μm diamond paste.

In order to observe both magnon and phonon scattering with a wider range of laser frequencies than in conventional Fabry-Perot spectroscopy, a SOPRA DMDP2000 Raman spectrometer was used. This double monochromator has a high resolution and a high rejection of stray light at low-frequency shifts.[8]

The pseudo-Brewster angle backscattering arrangement was adopted in the experiments, where the incident light is close to Brewster's angle (the angle of incidence was fixed at 67°) with the (001) surface, while the scattering light is collected at 90° to the incident one. Most of the visible laser wavelengths of both Ar^+ and Kr^+ lasers were used to study the excitation-wavelength dependence of the scattering. The incident laser power on the sample surface was kept at 100 mW. No apparent damage to the sample or variation of the recorded spectra were observed due to the laser heating. A compact permanent magnet of our own design was used to apply a magnetic field orthogonal to the light-scattering plane (i.e., along a $\langle 110 \rangle$ direction). The highest available magnetic field from the 3 cm diameter Nd-B-Fe pole pieces was 1.108 T at a gap width of 2.6 mm.

III. RESULTS AND DISCUSSION

Figure 1 shows the recorded spectra at various wavelengths for an applied magnetic field of 1.1 T, and Fig. 2 shows the wave-vector dependence of the frequency of the recorded peaks. The wave vector of the excitation was determined from the known refractive index of Bi-YIG (Ref. 3) and the light-scattering geometry. Two groups of Stokes and anti-Stokes peaks noted as M and P, respectively, are identified in Fig. 1. The single peak marked with X is an instrumental ghost line. With a decrease of the laser wavelength, the frequency shift of the peak P increases and a direct linear relationship between

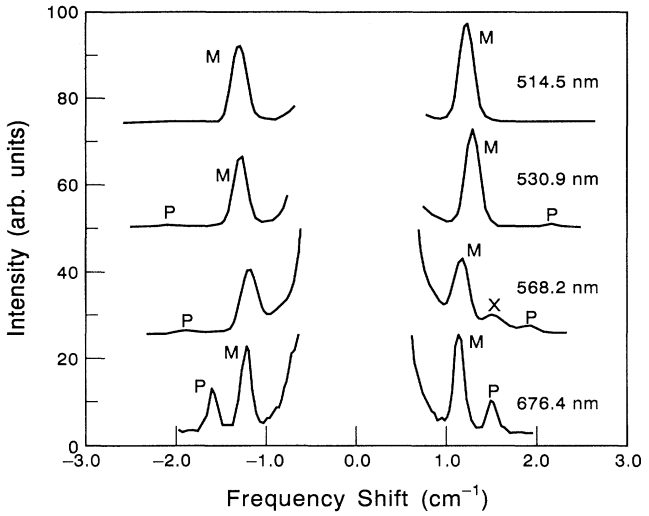

FIG. 1. Phonon and magnon light-scattering spectra of single crystal $Bi_{0.41}Y_{2.59}Fe_5O_{12}$ in an applied magnetic field of 1.108 T for different laser excitation wavelengths. The incident light was polarized in the scattering plane and the scattered light was recorded without analysis of its polarization. The spectral resolution was ~ 0.15 cm^{-1}. The spectra demonstrate the reduction of the phonon intensities due to sample absorption while the absorption-corrected magnon intensities are, in fact, increased with decreasing excitation wavelength.

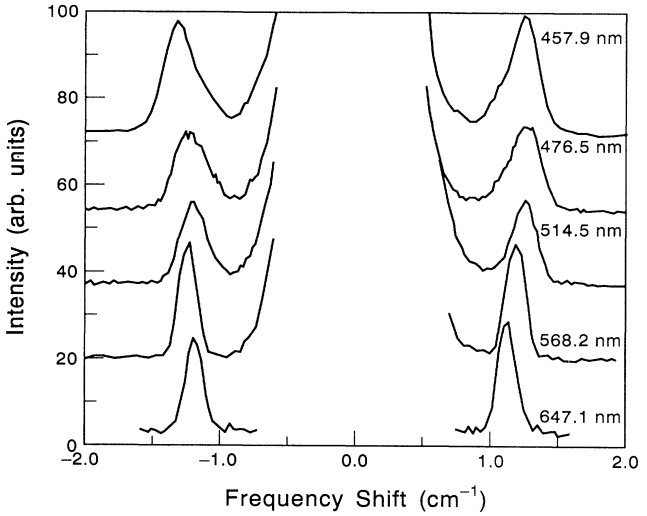

FIG. 3. The linewidth broadening and the asymmetric line shape of the magnon scattering measured with an applied field of 1.108 T at different laser wavelengths. The spectral resolution was ~ 0.15 cm^{-1}.

the shift and the scattering wave vector is observed. Hence, we conclude that these peaks are due to light scattering from phonons, and a further study of the scattered light polarization showed that they are the longitudinal-acoustic phonons. However, the intensity of peak P reduces sharply with an increase of the laser frequency and eventually is no longer observable. On the other hand, the frequencies of the Stokes and anti-Stokes peaks denoted by M do not increase so much with an increasing wave vector and they show a strong magnetic-field dependence. A scattered light polarization analysis confirmed that peak M is due to scattering from acoustic magnons. It appears from Fig. 1 that with the reduction of laser wavelength, the linewidth of the magnon peak becomes broader and broader. This can be seen more clearly in Figs. 3 and 4. Figure 3 demonstrates the broadening of the magnon linewidth with decreasing excitation wavelength and the appearance of an asymmetry in the line

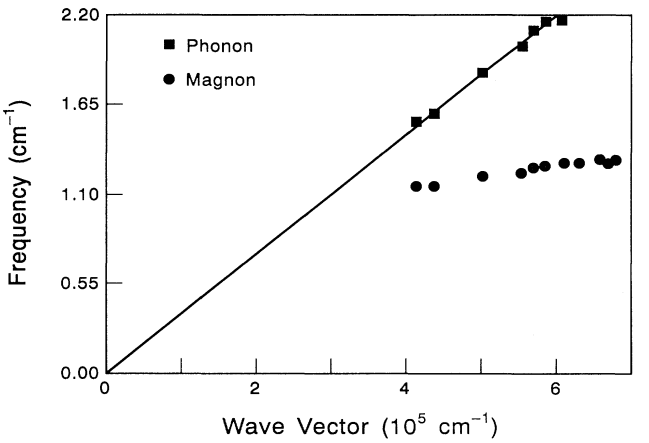

FIG. 2. The phonon and magnon dispersion relations obtained in the light-scattering measurements with an applied field of 1.108 T (see Fig. 1). The solid line is the theoretical fit to the longitudinal-acoustic-phonon dispersion [see Eq. (1)]. The theoretical fit to the magnon dispersion is shown in Fig. 5.

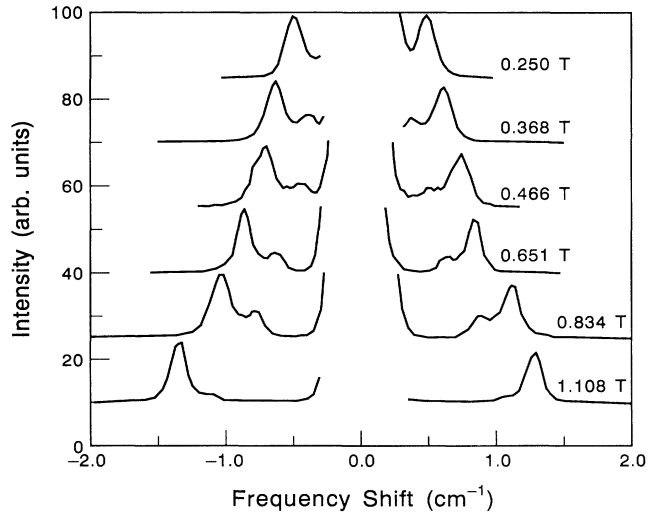

FIG. 4. Magnetic-field dependence of the magnon frequency in Bi-YIG as measured using 457.9 nm laser excitation and a spectral resolution of 0.08 cm^{-1}. Note the additional small peaks to lower frequency, which are now resolved in this higher-resolution measurement.

shape of the magnon peak at even shorter laser wavelengths. Figure 4 shows results obtained at higher resolution for 457.9 nm laser excitation with different applied magnetic fields, where a double peak line shape with a continuous band in between is now evident. The whole structure shifts to higher frequency when the magnetic field is increased. This clearly shows that the small peak near the main magnon peak is not due to a possible resonant crossover with a transverse-acoustic phonon, which is calculated to lie close to the magnon frequency for blue laser wavelengths and for applied fields ~ 1 T, but rather is magnetic in origin.

In Fig. 2, the measured phonon frequencies ω_p are well described by the usual linear dispersion relationship

$$\omega_p = v q_p \ , \tag{1}$$

where v is the sound velocity. The phonon wave vector q_p involved in the scattering process is given by

$$q_p = \frac{2\pi}{\lambda} n \left\{ \cos\left[\frac{\pi}{2} - \theta_B \right] + \cos\left[\sin^{-1}\left[\frac{\sin\theta_B}{n} \right] \right] \right\} , \tag{2}$$

where n is the refractive index,[3] λ the laser wavelength, and θ_B the Brewster angle (in this experiment we set $\theta_B = 67.0°$, fixed for the different wavelengths, although, strictly speaking, it should be changed slightly with the change in the incident laser wavelength). The sound velocity obtained in the fitting is $v = 6.851 \times 10^5$ cm/s for the longitudinal-acoustic phonon propagating in the (001) direction. On comparison with the corresponding value in pure YIG (Ref. 9) ($v = 7.215 \times 10^5$ cm/s) it is found that the elastic constant of YIG is reduced by the substitution of Y with Bi. Such a result is consistent with the large atomic mass change on going from Y (atomic mass 89) to Bi (atomic mass 209).

The magnon dispersion relation in a bulk ferrimagnet may be expressed as follows:[10]

$$\omega_m = \gamma \{ [B + (N_y - N_z) M_s + D q_m^2][B + (N_x - N_z) M_s + D q_m^2] \} \ , \tag{3}$$

where ω_m is the magnon frequency, γ the gyromagnetic ratio, B the applied magnetic field, N_x, N_y, and N_z are the sample demagnetization factors (with x along $\langle 001 \rangle$ and y and z along $\langle 110 \rangle$ directions), M_s the saturation magnetization, D the spin-wave stiffness constant, and q_m the magnon wave vector involved in the scattering process, which is the same as that for the phonon, as given in Eq. (2).

The shape of the sample is nearly cubic, $N_x \approx N_y \approx N_z$, but we do not know the demagnetization factors exactly. However, at a high applied magnetic field along z, the M_s related term is relatively small, and Eq. (3) may be written as

$$\omega_m = \gamma (B + N M_s + D q_m^2) \ , \tag{4}$$

where $N \approx N_x - N_z \approx N_y - N_z$. Equation (4) predicts a linear relationship between the magnon frequency and the applied magnetic field B and also the magnon wave vector squared q_m^2. This is proved to be the case by our experiments, as shown in Fig. 5 for the magnetic-field dependence measured with excitation at 457.9 nm and in Fig. 6 for the wave vector dependence measured with an applied field of 1.108 T. In the self-consistent fits to the data of Figs. 5 and 6, we obtained $\gamma = 28$ GHz/T, $D = 6.20 \times 10^{-13}$ T cm^2, and $NM_S = 25$ mT.

The increase of $D_{\rm YIG} = 5.4 \times 10^{-13}$ T cm^2 in pure YIG (Ref. 11) with the substitution of magnetic ions with diamagnetic Bi^{3+} ions is a very interesting result, and was also seen in earlier Brillouin scattering experiments[4] on other Bi-YIG samples. The composition dependence of D is shown in Fig. 7, and our result agrees very well with the earlier measurements. Although there have been many light-scattering studies of the effects of dilution with nonmagnetic ions on the magnetic excitations of antiferromagnets, we know of only one such study in a ferrimagnet.[5] From a Brillouin scattering study of zinc-substituted lithium ferrite $(Zn_xFe_{1-x})(Li_{(1-x)/2}Fe_{(3+x)/2})O_4$, Wilber, Kabos, and Patton[12] found that, for a given applied field, the magnon frequency decreased with increasing Zn content, while the spin-wave stiffness decreased rapidly to reach zero near $x = 0.4$. Clearly, in lithium ferrite the addition of Zn disrupts the Fe^{2+}-Fe^{2+} magnetic ion exchange interaction, reducing T_C and the exchange parameter in the process. This parallels the behavior found in antiferromagnets, for which there are a number of theories.[5] The behavior in Bi-YIG is *opposite* to this general trend, contrary to the predictions of existing theories. The experimental results of Fig. 7 when least-squares fitted to a straight line yield

$$D = D_{\rm YIG}(1 + 0.39x) \tag{5}$$

for the Bi concentration dependence of the spin-wave stiffness.

The only way to explain the contrary behavior in Bi-YIG is to assume that at least for small Bi concentrations ($x < 0.6$) the diamagnetic Bi^{3+} ions substitute only for

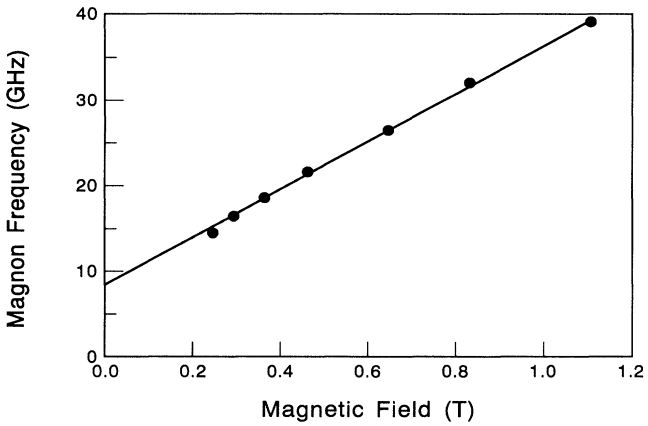

FIG. 5. Magnetic-field dependence of the magnon frequencies in Bi-YIG for 457.9 nm excitation: experiment (points) and theory (solid line).

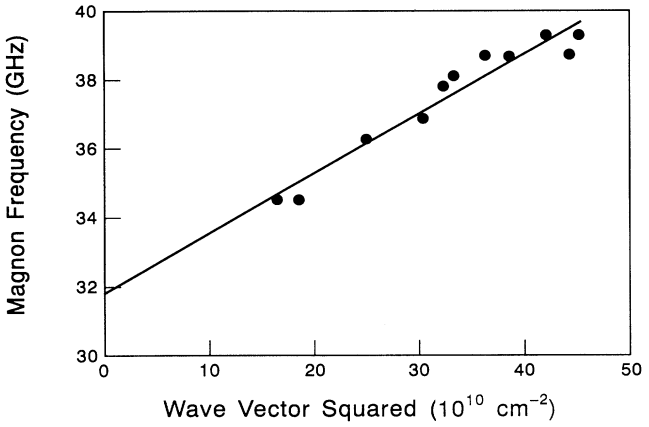

FIG. 6. Wave vector dependence of the magnon frequencies in Bi-YIG: experiment (points) and theory (solid line). The applied magnetic field was 1.108 T.

the magnetic Y^{3+} ions in YIG. Thus, to first order, the significant Fe^{3+}-Fe^{3+} magnetic ion exchange interactions are not affected by the substitution and D would also not be affected. Although Bi could replace either Y or Fe from an ionic charge point of view, such a single-ion substitution would be reasonable given that Y^{3+} and Bi^{3+} ions have larger ionic radii (0.89 and 0.96 Å, respectively) compared with Fe^{3+} ions (0.64 Å) and that the Y^{3+} ion site in YIG is surrounded by a much larger oxygen cage than the Fe^{3+} ion site. The fact that D actually *increases* with x could be due to a decrease in the superexchange path distance between nearest-neighbor Fe^{3+} ions via an intervening O^{2-} ion owing to the "squeezing" effect of neighboring large Bi^{3+} ions. However, another more likely explanation at low Bi concentrations is some modification of the bonding between the O^{2-} ions and the cations that enhances the Fe^{3+}-Fe^{3+} ion superexchange.

The reduction in scattering intensity of the LA phonon

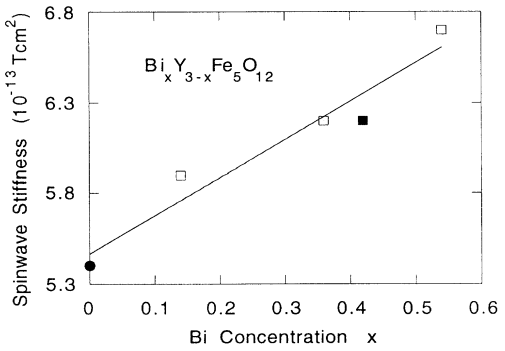

FIG. 7. The observed linear increase of the spin-wave stiffness constant D with the fraction x of Bi in $Y_{3-x}Bi_xFe_5O_{12}$: the experimental data are from Ref. 11 for pure YIG (solid circle), and from Ref. 4 (open squares) and this work (solid square) for doped YIG. The solid line is the result of a least-squares fit of a straight line to the data.

with decreasing wavelength, as shown in Fig. 1, is explained by the concomitant increase in the sample light absorption.[3] In marked contrast, on allowing for this sample absorption, the intensity of the magnon increases sharply with shorter wavelength excitation. This means that the incident light is very strongly coupled to the acoustic magnons, which is consistent with the fact that the Faraday rotation is strongly increased in Bi-YIG at shorter wavelengths.[3] This result could be used to help assign the electronic transitions in Bi-YIG, where in the visible many electronic transitions are observed, leading to difficulties in assigning them. Raman spectra of the sample measured with excitation at the shorter wavelengths on a Spex 14018 double monochromator show that the optic phonons are quite strong in intensity, while the optic magnons are very difficult to observe.[13] Thus, the mechanisms governing the coupling between the incident light and these various vibrational and magnetic excitations are very different.

The Stokes and anti-Stokes intensities of the acoustic magnon are essentially equal for blue excitation wavelengths (see Figs. 3 and 4), but become unequal with green-red excitation (see Fig. 1). Generally speaking, this is the same overall behavior as found for pure YIG (Ref. 6) and thus, the same conclusion likely applies, i.e., quadratic magneto-optic coupling of the light to the acoustic magnon becomes important at the longer excitation wavelengths. However, in detail, there are important differences between the Bi-YIG and pure YIG results in that the Stokes to anti-Stokes intensity ratio for Bi-YIG never shows the same disparity in the red as in pure YIG and the wavelength dependences of the scattered-light intensity are quite different. Both of these major differences can be attributed to Bi-induced changes in the magneto-optical parameters of YIG.

Another interesting result from these experiments is the wavelength dependence of the linewidth of the magnon scattering. From Fig. 3 it is apparent that with decreasing excitation wavelength, the linewidth of the magnon peak becomes broader and broader, and also becomes asymmetric. Figure 4 shows higher-resolution measurements at 457.9 nm, where the sample absorption is highest, and with different applied magnetic fields. It is clear that the asymmetric line shape is, in fact, derived from two peaks, and both of them shift by approximately the same amount with a change in the applied magnetic field. Hence, the additional small peak to lower frequency is of magnetic origin and is related to the main acoustic magnon peak. Similar spectra have been observed in Brillouin scattering from magnons in Bi-Ca-VIG single crystals (where VIG stands for vanadium iron garnet).[14] In those experiments, the small additional peak is asymmetric, and between the bulk magnon peak and this small peak there is a continuum band. These features also shift together with a change in the applied magnetic field. Here, for Bi-YIG, the light-scattering spectra are recorded using a SOPRA DMDP2000 spectrometer, which has a high-resolution capability, but the resolution is still low compared to a Fabry-Perot interferometer. Hence, the difference in the appearance of the spectra for the two types of garnet likely originates from the different resolu-

TABLE I. Observed and calculated additional weak peak frequencies ω_2 for 457.9 nm excitation and with different applied magnetic field B (see Fig. 4). For further details see the text.

B (T)	Measured ω_2 (GHz)	Calculated ω_2 (GHz)
0.368	11.99	11.56
0.466	14.39	14.31
0.651	19.49	19.49
0.834	25.48	24.60
1.108	32.40	32.30

tion capabilities of the two spectrometers. Since these additional weaker peaks are observed for excitation in a high light-absorption wavelength region, they are possibly due to the wave vector uncertainty in the surface region of the sample. If this is true, then the additional small peaks should correspond to the smallest available wave vector, which, in our case, is the surface component $q_{\parallel}$ of the incident and scattered light wave vectors:

$$q_{\parallel}=\frac{2\pi}{\lambda}\left[\sin\theta_B+\sin\left[\frac{\pi}{2}-\theta_B\right]\right], \tag{6}$$

which is 1.8×10^5 cm^{-1} for $\lambda=457.9$ nm. Substitution of q_m with $q_{\parallel}$ in Eq. (4) allows predictions of the frequency of these additional peaks at different applied magnetic fields. Table I compares the results of the measurements and this calculation (all other parameter values used in the calculation are the same as those obtained earlier). The agreement is very good.

IV. CONCLUSIONS

Light-scattering spectroscopy of Bi-substituted YIG has shown that the intensity versus wavelength dependences are very different for acoustic phonons and magnons. The intensities of the acoustic magnons are resonantly enhanced at blue excitation wavelengths, while that for the acoustic phonons are reduced due to the high light absorption in the sample. At the same time, the optic phonons show only a weak dependence on the laser wavelength, and the optic magnons are still very difficult to observe. These results have significance for the study of the light coupling to the phonons and magnons in pure and impure garnets, as well as the nature of the electronic transitions involved.

The observed increase of the spin-wave stiffness constant in YIG due to the doping with Bi has proved that diamagnetic Bi^{3+} ions substitute for magnetic Y^{3+} ions and not only influence but also *enhance* the magnetic properties of the materials. The mechanism of this unusual effect is probably due to the large spin-orbit coupling, and subsequent mixing, of the $6p$ orbital of Bi^{3+} ions with the $2p$ orbital of O^{2-} ions. The substitution of Y with Bi softens the crystal, because the measured sound velocity is smaller than that in pure YIG. The magnon double peak and the peculiar line shape observed at shorter laser wavelengths is most likely due to wave vector nonconservation, because of the high light absorption of the sample at these wavelengths. If so, then the observed line shape will yield information on the density of states of the spin waves for small wave vectors and on the pinning of spin waves at the surface.

*On leave from Institute of Physics, Chinese Academy of Sciences, Beijing, China.

[1]K. Matsumoto, S. Sasaki, Y. Asahara, K. Yamaguchi, and T. Fujii, J. Magn. Magn. Mater. **104-107**, 451 (1992).
[2]T. Hirano, J. Appl. Phys. **70**, 6292 (1991).
[3]V. Doormann, J.-P. Krumme, and C.-P. Klages, Appl. Phys. A **34**, 223 (1984).
[4]Y. L. Liu, P. X. Zhang, Y. J. Mo, and A. Tu, Acta Phys. Sin. **36**, 651 (1987).
[5]M. G. Cottam and D. J. Lockwood, *Light Scattering in Magnetic Solids* (Wiley, New York, 1986).
[6]W. Wettling, M. G. Cottam, and J. R. Sandercock, J. Phys. C **8**, 211 (1975).
[7]X. Z. Xu, W. Y. Jia, and C. X. Liu, Acta Phys. Sin. **29**, 1558 (1980).
[8]P. X. Zhang, D. J. Lockwood, H. J. Labbé, and J.-M. Baribeau, Phys Rev. B **46**, 9881 (1992).
[9]V. F. Kitaeva, V. E. Zharikov, and I. L. Chistyi, Phys. Status Solidi A **92**, 475 (1985).
[10]H. Suhl, J. Phys. Chem. Solids **1**, 209 (1957).
[11]J. R. Sandercock and W. Wettling, Solid State Commun. **13**, 1729 (1973).
[12]W. D. Wilber, P. Kabos, and C. E. Patton, IEEE Trans. Magn. **MAG-19**, 1862 (1983).
[13]P. X. Zhang, D. J. Lockwood, and H. J. Labbé (unpublished).
[14]P. X. Zhang, Y. Z. Pang, and G. Guntherodt, J. Magn. Magn. Mater. **86**, 296 (1990).